



Calhoun: The NPS Institutional Archive
DSpace Repository

Theses and Dissertations

1. Thesis and Dissertation Collection, all items

1961

A study of geostrophic angular momentum
transport by waves with period 1 to 30 days
at the 500-mb surface and a mid-latitude station

Blaes, Carl E.

Monterey, California: U.S. Naval Postgraduate School

<http://hdl.handle.net/10945/13160>

Downloaded from NPS Archive: Calhoun



Calhoun is the Naval Postgraduate School's public access digital repository for research materials and institutional publications created by the NPS community. Calhoun is named for Professor of Mathematics Guy K. Calhoun, NPS's first appointed -- and published -- scholarly author.

Dudley Knox Library / Naval Postgraduate School
411 Dyer Road / 1 University Circle
Monterey, California USA 93943

<http://www.nps.edu/library>

NPS ARCHIVE
1961
BLAES, C.

A STUDY OF GEOSTROPHIC ANGULAR MOMENTUM
TRANSPORT BY WAVES WITH PERIODS 1 TO 30
DAYS AT THE 500-MB SURFACE AND
A MID-LATITUDE STATION

CARL E. BLAES

LIBRARY
U.S. NAVAL POSTGRADUATE SCHOOL
MONTEREY, CALIFORNIA



29.2



A STUDY OF GEOSTROPHIC ANGULAR MOMENTUM
TRANSPORT BY WAVES WITH PERIODS 1 TO 30
DAYS AT THE 500-MB SURFACE AND A MID-LATITUDE STATION

* * * * *

Carl E. Blaes

THE UNIVERSITY OF CHICAGO
LIBRARY
1100 EAST 58TH STREET
CHICAGO, ILLINOIS 60637

10/10/10

A STUDY OF GEOSTROPHIC ANGULAR MOMENTUM
TRANSPORT BY WAVES WITH PERIODS 1 TO 30
DAYS AT THE 500-MB SURFACE AND A MID-LATITUDE STATION

by

Carl E. Blaes
"

Lieutenant Commander, United States Navy

Submitted in partial fulfillment of
the requirements for the degree of

MASTER OF SCIENCE

IN

METEOROLOGY

United States Naval Postgraduate School
Monterey, California

1 9 6 1

NPS ARCHIVE

1961

BLAES, C.

Thesis

~~PC 457~~

ABSTRACT

The winter-time transport of geostrophically computed angular momentum at 500 mb for the period 1 December 1955 to 28 February 1956 is obtained for Sault Ste. Marie, Michigan. This transport is subjected to a cospectral analysis to compute the contribution of harmonic waves with periods 1 - 30 days to the total angular momentum transport. Computations are made for two other stations, one east, and one south of Sault Ste. Marie for comparison of transport as related to general circulation processes.

The author is deeply indebted to Professor F. L. Martin, Department of Meteorology, U.S. Naval Postgraduate School, for his encouragement and invaluable aid in the preparation of this manuscript.

TABLE OF CONTENTS

Section	Title	Page
1.	Introduction	1
2.	Mathematical Formulations	2
3.	General Procedures	8
4.	Limitations and Sources of Error	10
5.	Interpretation of Cospectra	15
6.	Conclusions	19
7.	Bibliography	23
8.	Appendix I	24

LIST OF ILLUSTRATIONS

Figure		Page
1.	Illustration of χ^2/v test of significance at the 95% level of belief	12
2.	Illustration of the effects of sampling variations in giving an aliased spectrum	12
3.	The cospectrum of the mean relative angular momentum transport at the 500-mb level over Sault Ste. Marie, Michigan, for the period 1 December 1955 through 28 February 1956	20
4.	The cospectrum of the mean relative angular momentum transport at the 500-mb level over Caribou, Maine, for the period 1 December 1955 through 28 February 1956	21
5.	The cospectrum of the mean relative angular momentum transport at the 500-mb level over Caribou, Maine, for the period 1 December 1954 through 28 February 1955	21
6.	The cospectrum of the mean relative angular momentum transport at the 500-mb level over Athens, Georgia, for the period 1 December 1955 through 28 February 1956	22

TABLE OF SYMBOLS

Symbol	Definition
M	absolute angular momentum per unit mass
u	zonal component of the wind
v	meridional component of the wind
λ	linear distance along a parallel of latitude
y	linear distance along a meridian
g	acceleration due to gravity
r	radius of the earth
ρ	density of air
f	coriolis parameter
ΔX	grid length along a parallel of latitude
ΔY	grid length along a meridian
N	total observations
u_g	geostrophic wind component along a parallel of latitude
v_g	geostrophic wind component along a meridian
ΔZ_λ	increment of contour height along a parallel of latitude
ΔZ_y	increment of contour height along a meridian
Δp	increment of pressure equal to one millibar

Symbol	Definition
$\Delta \lambda$	increment equal to one centimeter of length along a parallel of latitude
$S(\tau)$	mean cross covariance of two continuous functions of time
τ	lag applied to a continuous function
$u(t)$	time series of the wind component along a parallel of latitude
$v(t)$	time series of the wind component along a meridian
Γ	averaging period
$g_u(h)$	Fourier transform of $u(t)$
$\hat{g}_v(h)$	complex conjugate of the Fourier transform of $v(t)$
n	harmonic number
C_n	cospectral estimate
T	fundamental period
ω	angular velocity
m	maximum lag
Δt	increment of time
k	integer of lag
S_k	mean cross covariance of two discrete functions of time

Symbol	Definition
f_n	frequency
$\chi^2_{.05}$	chi-square value at the 5% level
\bar{P}	mean cospectral value between peak and trough of the cospectrum
ν	degrees of freedom
f_m	Nyquist frequency

1. Introduction

Widger [10] in his study of the flow of absolute angular momentum in the atmosphere stated:

Although even a complete knowledge of the angular momentum transfer in the atmosphere cannot by itself furnish a solution of the problem of the general circulation, any proposed scheme for this circulation should include a means for securing the angular momentum flows which are observed. For this reason, it is essential that all possible observational knowledge concerning these processes be obtained.

Many authors in recent years, Widger, Starr, and Mintz [10, 7, 3] for example, have provided studies in connection with the relationship of the absolute angular momentum transport to the general circulation, or the global balance of angular momentum. In general these studies provide quantitative findings of the spatial distribution of the total momentum transport and establish the fact that there is a mean poleward transport.

This paper, in hopes of contributing to the knowledge of angular momentum transport, has as its purpose a cospectral analysis of the angular momentum transport for waves of periods 1 - 30 days. Due to the limited time available for the study, it was confined to the 500-mb level at a station in the mid-latitudes. The primary station employed was Sault Ste. Marie, Michigan.

Several other cospectra are included for other stations for the purpose of comparison. However, the spectrum for these comparative stations are for periods 2 - 30 days.

Received of the Hon. Secy. of the Navy

the sum of \$100.00

for the purchase of the following articles
viz 100 lbs of sugar 100 lbs of coffee
100 lbs of rice 100 lbs of flour
100 lbs of beans 100 lbs of peas
100 lbs of lentils 100 lbs of corn
100 lbs of wheat 100 lbs of barley
100 lbs of oats 100 lbs of rye
100 lbs of buckwheat 100 lbs of millet
100 lbs of sorghum 100 lbs of amaranth
100 lbs of quinoa 100 lbs of buckwheat
100 lbs of millet 100 lbs of sorghum
100 lbs of amaranth 100 lbs of quinoa

for the purchase of the following articles

viz 100 lbs of sugar 100 lbs of coffee
100 lbs of rice 100 lbs of flour
100 lbs of beans 100 lbs of peas
100 lbs of lentils 100 lbs of corn
100 lbs of wheat 100 lbs of barley
100 lbs of oats 100 lbs of rye
100 lbs of buckwheat 100 lbs of millet
100 lbs of sorghum 100 lbs of amaranth
100 lbs of quinoa 100 lbs of buckwheat
100 lbs of millet 100 lbs of sorghum
100 lbs of amaranth 100 lbs of quinoa

for the purchase of the following articles
viz 100 lbs of sugar 100 lbs of coffee
100 lbs of rice 100 lbs of flour
100 lbs of beans 100 lbs of peas
100 lbs of lentils 100 lbs of corn
100 lbs of wheat 100 lbs of barley
100 lbs of oats 100 lbs of rye
100 lbs of buckwheat 100 lbs of millet
100 lbs of sorghum 100 lbs of amaranth
100 lbs of quinoa 100 lbs of buckwheat
100 lbs of millet 100 lbs of sorghum
100 lbs of amaranth 100 lbs of quinoa

for the purchase of the following articles
viz 100 lbs of sugar 100 lbs of coffee
100 lbs of rice 100 lbs of flour
100 lbs of beans 100 lbs of peas
100 lbs of lentils 100 lbs of corn
100 lbs of wheat 100 lbs of barley
100 lbs of oats 100 lbs of rye
100 lbs of buckwheat 100 lbs of millet
100 lbs of sorghum 100 lbs of amaranth
100 lbs of quinoa 100 lbs of buckwheat
100 lbs of millet 100 lbs of sorghum
100 lbs of amaranth 100 lbs of quinoa

2. Mathematical Formulations

Widger [10] has shown that the rate at which the absolute angular momentum of the zonal wind is increasing in a portion of the atmosphere bounded by the earth's surface, the top of the atmosphere and extending from the pole to a given latitude ϕ may be expressed as

$$\frac{\partial}{\partial t} \int \rho M dV = \int \rho M V_n dS + \int p r d\sigma + \int r \tau_A dS \quad (1)$$

where dV is any element of volume within the polar cap just described, dS an element of the surface of the volume, $d\sigma$ the projection of an element of the earth's surface area on the meridional plane passing through a given point, p is the pressure, r the radius of the earth, and τ_A the eastward frictional stress acts only on the air at the earth's surface.

In the first term on the right V_n is the meridional component v of the velocity into the polar cap. Since the vertical velocities at the earth's surface and top of the atmosphere may both be considered zero, this quantity as a whole represents the rate at which angular momentum is brought into the region by air motion across the boundary. The second and third terms on the right represent, respectively, the rate at which angular momentum is changed due to the torque exerted by pressure differentials across mountain ranges and the westward torque, $r\tau_A$, exerted by frictional drag at the earth's surface. However, since this study will consider only the transport through a unit area of the

latitude wall at the 500-mb surface, the terms involving pressure and friction torques may be neglected. No attempt is made herein to determine the left side of equation (1) from the computed transport at 500 mb.

The absolute angular momentum of a gram of air at latitude ϕ may be written

$$M = ur \cos \phi + \Omega r^2 \cos^2 \phi \quad (2)$$

Furthermore, since $V_n = \bar{v}$ and the element of surface may be taken as an element of the latitude wall, $dS = d\lambda dz$, taking the first term on the right in equation (1), the transport of absolute angular momentum may be written as the sum of two terms,

$$r \cos \phi \iint \rho u \bar{v} d\lambda dz \quad (3)$$

equal to the rate of advection of "relative" angular momentum, and the Ω -momentum defined as

$$\Omega r^2 \cos^2 \phi \iint \rho \bar{v} d\lambda dz \quad (4)$$

which is equal to the rate of advection of angular momentum due to the earth's rotation. Since Ω -momentum does not lend itself to a cospectral analysis and will not be computed in this study, the chief emphasis is placed upon the average angular momentum transport through a unit area and per unit time given by equation (3). Therefore, after applying the geostrophic approximation for u and \bar{v} in equation (3) and dividing by N , one obtains the average angular momentum transport

$$\frac{g r \cos \phi}{f^2 (\Delta x)^2 N} \left(\sum \Delta z_x \Delta z_y \right) \Delta x \Delta p \quad (5)$$

where the hydrostatic equation has also been used in (3).

At first glance equation (5) appears to be a summation of N terms around the latitude circle at a distance Δx apart, and thus a representation of equation (3). However, a slightly different interpretation was placed upon equation (5), in that Δx represents a grid distance of 300 nautical miles centered on the station for which the computation is being made, and Δz_x and Δz_y are the contour-height increments defining the mean geostrophic wind components

$$u_g = -\frac{g}{f} \frac{\Delta z_y}{\Delta y} \quad \text{and} \quad v_g = \frac{g}{f} \frac{\Delta z_x}{\Delta x} \quad (6)$$

in the neighborhood of the station. In addition, Δy was taken equal to Δx in equation (6). Thus the interpretation of equation (5) actually employed here was to regard it as a time-average, over N equal time intervals, of values of relative angular momentum transport centered at the station. The vertical increment for convenience was taken as Δp equal to one millibar and Δx on the right side of equation (5) was scaled down to one centimeter instead of the equivalent length of 300 nautical miles used for the grid. The units of angular momentum transport in this study will then be $\text{cm}^3\text{-mb}$.

Equation (5) shows that the geostrophic relative momentum transport depends upon the cross covariance between

$$f(x) = \frac{1}{2} \left(1 + \frac{x}{\sqrt{1+x^2}} \right)$$

Let $f(x)$ be a function defined on \mathbb{R} by $f(x) = \frac{1}{2} \left(1 + \frac{x}{\sqrt{1+x^2}} \right)$. Show that f is a bijection from \mathbb{R} to $(0, 1)$.

Let $f(x) = \frac{1}{2} \left(1 + \frac{x}{\sqrt{1+x^2}} \right)$. Show that f is a bijection from \mathbb{R} to $(0, 1)$. To show that f is injective, suppose $f(x) = f(y)$. Then $\frac{1}{2} \left(1 + \frac{x}{\sqrt{1+x^2}} \right) = \frac{1}{2} \left(1 + \frac{y}{\sqrt{1+y^2}} \right)$. This implies $\frac{x}{\sqrt{1+x^2}} = \frac{y}{\sqrt{1+y^2}}$. Squaring both sides gives $\frac{x^2}{1+x^2} = \frac{y^2}{1+y^2}$, which simplifies to $x^2(1+y^2) = y^2(1+x^2)$. This further simplifies to $x^2 + x^2y^2 = y^2 + x^2y^2$, which implies $x^2 = y^2$. Since f is increasing, we have $x = y$.

To show that f is surjective, let $y \in (0, 1)$. We need to find $x \in \mathbb{R}$ such that $f(x) = y$. This means $\frac{1}{2} \left(1 + \frac{x}{\sqrt{1+x^2}} \right) = y$, which implies $\frac{x}{\sqrt{1+x^2}} = 2y - 1$. Squaring both sides gives $\frac{x^2}{1+x^2} = (2y-1)^2$, which simplifies to $x^2 = (2y-1)^2(1+x^2)$. This further simplifies to $x^2(1 - (2y-1)^2) = (2y-1)^2$. Since $1 - (2y-1)^2 > 0$, we have $x^2 = \frac{(2y-1)^2}{1 - (2y-1)^2}$. Taking the square root gives $x = \frac{2y-1}{\sqrt{1 - (2y-1)^2}}$. This shows that for every $y \in (0, 1)$, there exists an $x \in \mathbb{R}$ such that $f(x) = y$.

$$f(x) = \frac{1}{2} \left(1 + \frac{x}{\sqrt{1+x^2}} \right)$$

Let $f(x) = \frac{1}{2} \left(1 + \frac{x}{\sqrt{1+x^2}} \right)$. Show that f is a bijection from \mathbb{R} to $(0, 1)$. To show that f is injective, suppose $f(x) = f(y)$. Then $\frac{1}{2} \left(1 + \frac{x}{\sqrt{1+x^2}} \right) = \frac{1}{2} \left(1 + \frac{y}{\sqrt{1+y^2}} \right)$. This implies $\frac{x}{\sqrt{1+x^2}} = \frac{y}{\sqrt{1+y^2}}$. Squaring both sides gives $\frac{x^2}{1+x^2} = \frac{y^2}{1+y^2}$, which simplifies to $x^2(1+y^2) = y^2(1+x^2)$. This further simplifies to $x^2 + x^2y^2 = y^2 + x^2y^2$, which implies $x^2 = y^2$. Since f is increasing, we have $x = y$.

To show that f is surjective, let $y \in (0, 1)$. We need to find $x \in \mathbb{R}$ such that $f(x) = y$. This means $\frac{1}{2} \left(1 + \frac{x}{\sqrt{1+x^2}} \right) = y$, which implies $\frac{x}{\sqrt{1+x^2}} = 2y - 1$. Squaring both sides gives $\frac{x^2}{1+x^2} = (2y-1)^2$, which simplifies to $x^2 = (2y-1)^2(1+x^2)$. This further simplifies to $x^2(1 - (2y-1)^2) = (2y-1)^2$. Since $1 - (2y-1)^2 > 0$, we have $x^2 = \frac{(2y-1)^2}{1 - (2y-1)^2}$. Taking the square root gives $x = \frac{2y-1}{\sqrt{1 - (2y-1)^2}}$. This shows that for every $y \in (0, 1)$, there exists an $x \in \mathbb{R}$ such that $f(x) = y$.

Let $f(x) = \frac{1}{2} \left(1 + \frac{x}{\sqrt{1+x^2}} \right)$. Show that f is a bijection from \mathbb{R} to $(0, 1)$. To show that f is injective, suppose $f(x) = f(y)$. Then $\frac{1}{2} \left(1 + \frac{x}{\sqrt{1+x^2}} \right) = \frac{1}{2} \left(1 + \frac{y}{\sqrt{1+y^2}} \right)$. This implies $\frac{x}{\sqrt{1+x^2}} = \frac{y}{\sqrt{1+y^2}}$. Squaring both sides gives $\frac{x^2}{1+x^2} = \frac{y^2}{1+y^2}$, which simplifies to $x^2(1+y^2) = y^2(1+x^2)$. This further simplifies to $x^2 + x^2y^2 = y^2 + x^2y^2$, which implies $x^2 = y^2$. Since f is increasing, we have $x = y$.

To show that f is surjective, let $y \in (0, 1)$. We need to find $x \in \mathbb{R}$ such that $f(x) = y$. This means $\frac{1}{2} \left(1 + \frac{x}{\sqrt{1+x^2}} \right) = y$, which implies $\frac{x}{\sqrt{1+x^2}} = 2y - 1$. Squaring both sides gives $\frac{x^2}{1+x^2} = (2y-1)^2$, which simplifies to $x^2 = (2y-1)^2(1+x^2)$. This further simplifies to $x^2(1 - (2y-1)^2) = (2y-1)^2$. Since $1 - (2y-1)^2 > 0$, we have $x^2 = \frac{(2y-1)^2}{1 - (2y-1)^2}$. Taking the square root gives $x = \frac{2y-1}{\sqrt{1 - (2y-1)^2}}$. This shows that for every $y \in (0, 1)$, there exists an $x \in \mathbb{R}$ such that $f(x) = y$.

u_g and v_g . It therefore represents the average geostrophic relative angular momentum transported across a section of the latitude wall with grid length $\Delta\lambda = 1^\circ$ and vertical thickness $\Delta p = 1 \text{ mb}$.

The mean cross covariance $S(\tau)$ of two stationary, Gaussian time-series $u(t)$ and $v(t)$, at lag τ , may be expressed by the convolution integral

$$S(\tau) = \lim_{T \rightarrow \infty} \frac{1}{T} \int_0^T u(t) v(t+\tau) dt \quad (7)$$

Frequently in meteorological applications, $S(\tau)$ is "evenized" by forming the quantity

$$\frac{S(\tau) + S(-\tau)}{2} \quad (8)$$

which is independent of the sign of lag τ . Henceforth, it will be understood that the mean cross covariance has been evenized.

The cross-spectrum (or simply cospectrum) C_n of the two series $u(t)$ and $v(t)$ is defined as that part of the mean cross covariance associated with a unit wave band centered at wave number n in both series. In symbols C_n may then be defined as

$$C_n = \lim_{T \rightarrow \infty} \frac{g_u(n) \hat{g}_v(n)}{T} \quad (9)$$

where T is the averaging period and $g_u(n)$ and $g_v(n)$ are the Fourier transforms of $u(t)$ and $v(t)$ respectively, defined as in

$$g_n(u) = \lim_{T \rightarrow \infty} \int_0^T u(t) e^{-i\omega t} dt \quad \omega = \frac{2\pi n}{T} \quad (10)$$

of the ...
...
...

...
...
...

...
...
...

...
...
...

...
...
...

...
...
...

...
...
...

The circumflex indicates the complex conjugate.

If one now employs the definition of cross covariance $S(\tau)$ for an evenized function, as contained in equation (7), the Faltung theorem leads to the Fourier integral expression

$$S(\tau) = \lim_{T \rightarrow \infty} \int_0^T C(n) \cos \frac{2\pi n \tau}{T} dn \quad (11)$$

so that $S(\tau)$ and $C(n)$ are spoken of as Fourier-transform pairs. Equation (11) may be inverted to solve for C_n in terms of $S(\tau)$. Also, the resulting inversion can be specialized to the case of a finite, but long, averaging period Γ , giving

$$C(n) = 2 \int_0^\Gamma S(\tau) \cos \omega \tau d\tau \quad \omega = \frac{2\pi n}{T_{max}} \quad (12)$$

A proof of equation (12) is given, from first principles, in Appendix I.

When discrete data are employed at time intervals of Δt , using a maximum lag of $m\Delta t$, the maximum period, or fundamental, that can be resolved is

$$T_{max} = 2 m \Delta t \quad (13)$$

In equation (12), since τ appears as a summand, τ will be written as

$$\tau = k \Delta t \quad k = 0, 1, 2, \dots, m \quad (14)$$

with k taking on each of the discrete values shown in (14). Since the averaging period of equations (12) is $\Gamma = m\Delta t$, equation (12) leads to

$$C_n = \frac{2}{m} \left\{ \frac{1}{2} [S_0 + (-1)^n S_m] + \sum_{k=1}^{m-1} S_k \cos \frac{\pi n k}{m} \right\} \quad (15)$$

$$1 \leq n \leq m-1$$

In the case of C_0 and C_m , the resulting coefficients are divided by two, since only one-half bandwidth is available at $n=0$ and $n=m$. Combining equations (5), (7), and (8), the cross covariance for k lags is

$$S_k = \frac{gr \cos \phi}{2 f^2 (\Delta x)^2 (N-k)} \left(\sum_{i=1}^{N-k} \Delta z_{k,i} \Delta z_{k,i+k} + \Delta z_{k,i+k} \Delta z_{k,i} \right) \Delta A \Delta P \quad (16)$$

$$0 \leq k \leq m$$

since the averaging period of equation (7) is now $\Gamma = (N-k)\Delta t$. The factor two in the denominator of equation (16) results from evenizing.

The cospectral estimates offered by equation (15) are termed "raw estimates". Blackman and Tuxey [1] have suggested several smoothing procedures, the simplest of which involves application of a moving-weighted average defined by

$$\bar{C}_n = .25 C_{n-1} + .5 C_n + .25 C_{n+1} \quad (17)$$

In the case of $n=m$ there is no higher value to include in the average and the weighted average is modified so that

$$\bar{C}_m = .5 C_{m-1} + .5 C_m \quad (18)$$

مذكرة عن تاريخ مصر القديمة

أحمد حسن

المقدمة
تعد مصر من أقدم الحضارات في التاريخ، وقد شهدت ازدهاراً عظيماً في مختلف العصور. من خلال هذه المذكرة، سنستعرض أهم المراحل التاريخية التي شكلت مصر القديمة، من العصور الفرعونية إلى العصر البطلمي.

العصر الفرعوني القديم (3100 - 2686 ق.م)

أولاً

في هذا العصر، تأسست الدولة المصرية الأولى، وظهرت الحضارة المصرية القديمة.

من أهم إنجازات هذا العصر:

1- اكتشاف الزراعة والكتابة.

2- بناء الأهرامات العظيمة.

3- اكتشاف الطب والهندسة.

4- اكتشاف الفلك والموسيقى.

5- اكتشاف الفنون الجميلة.

6- اكتشاف الفلسفة والعلوم.

7- اكتشاف الأدب والفن.

8- اكتشاف التاريخ والجغرافيا.

9- اكتشاف الفلك والموسيقى.

10- اكتشاف الفلسفة والعلوم.

11- اكتشاف الأدب والفن.

12- اكتشاف التاريخ والجغرافيا.

3. General Procedures

The initial step required establishing what data were to be used in making computations. Recalling that the computed periods are determined by the relation $2m\Delta t/n$, where m is the maximum number of lags at discrete time intervals Δt , it is clear that a half-day lag interval requires 30 lags to obtain a spectrum for periods 1 - 30 days. On the other hand, a one-day sample and lag interval requires only 15 lags to obtain a spectrum for periods 2 - 30 days. However, Blackman and Tukey[1] state that the best results are obtained when the longest lag is about 5 - 10 per cent of the length of the record. This would require that the record, if possible, consist of 300 - 600 observations when using the 500-mb charts produced at 0300 GMT and 1500 GMT daily, or half this number when using only one series of charts. In order to obtain this number of observations, it would require a minimum of 5 months data and the spectrum would be influenced by seasonal regimes. In order to reduce the data-processing load and inter-annual influences as much as possible, it was decided to use the observations from the three winter months of December 1955, January 1956, and February 1956. Thus the longest lag was only 17 per cent of the length of the record for this particular season. However, no claim is made that the cospectra obtained are necessarily representative of those for other winter seasons.

Data were taken from two sources, depending on the station being considered. Since heights of both the 0300

GMT and 1500 GMT 500-mb level were required at Sault Ste. Marie, Michigan, the primary station studied in this paper, facsimile charts transmitted by the U. S. Weather Bureau were utilized. In the case of the other stations used for comparison, the smallest period computed was only two days and the data used were the 1500 GMT charts published in Daily Series Synoptic Weather Maps [8].

From the above-mentioned charts, the geopotential height differences were obtained with a 5.0 degree (latitude) grid. Assuming that normal synoptic smoothing was applied in preparation of the charts, a grid of this dimension should not filter out significant short waves that have not already been removed by synoptic smoothing.

In five cases, where the 0300 GMT facsimile charts were missing, geopotential height differences were computed from the actual observed wind listed in Northern Hemisphere Data Tabulations [9]. The observed winds were reduced to geostrophic values by subjectively compensating for the degree of cyclonic or anticyclonic curvature associated with the flow.

The smoothed cospectra of geostrophic relative angular momentum transport were obtained by using these data in equations (15), (16), (17), and (18), and are graphically displayed in figs. 3 through 6. All computations except for the final smoothing, utilizing equations (17), (18), were accomplished on the CDC - 1604 digital computer.

4. Limitations and Sources of Error

The computational results of this study have been based on discrete data using equal intervals Δt . In one series of computations, indicated by the solid line in fig. 3, the data interval was reduced to 12 hours in order to determine the effects of sampling fluctuations and of atmospheric oscillations. In all other cospectral analyses, the data interval was 24 hours. Throughout the study the maximum lag was 15 days.

The period associated with the smoothed cospectral estimate is $2m\Delta t/n$ with $n=1,2,\dots,m$. On the other hand the central frequency f_n of the frequency band is

$$f_n = \frac{n}{2m\Delta t} \quad n=1,2,\dots,m$$

and the highest frequency resolvable occurs for $n=m$; this frequency is called the Nyquist frequency f_m . The cospectral estimate corresponds to the frequency band

$$(n-1/2)/2m\Delta t \quad \text{to} \quad (n+1/2)/2m\Delta t$$

It should be noted that it is difficult to resolve frequencies contributing to the cospectrum at the longer periods. For example when $n=1$, the frequency band spans the range $1/20$ cycle / day to $1/60$ cycle / day.

In order to assess the reality of sharp peaks or troughs, Panofsky's criterion for χ^2/ν distribution of the power spectrum has been followed. Strictly speaking a much more rigorous method of assessing significance would have been achieved by testing the cospectral correlation

function defined by

$$R_{\cos}^2 = \frac{C_n^2}{P_{n,u} P_{n,v}}$$

Here C_n is the cospectral estimate for the n^{th} harmonic, and $P_{n,u}$ and $P_{n,v}$ are the power spectral estimates for u and v at the same harmonic. However, the power spectra computations were not available in time for the completion of this aspect of the work. Hence, the more qualitative approach indicated in fig. 1 was attempted with some misgivings. It must be emphasized that when the term "95% confidence limit" is used, it is only by analogy with corresponding phraseology to be found in Panofsky and Brier [4, p. 145]. The actual confidence may be at a somewhat lower level.

Applying the χ^2/ν distribution to the cospectrum, a peak or trough could not have happened randomly (at the 95% level of belief) provided the peak or trough in the cospectral estimate lies outside the range ΔP , defined as

$$\Delta P = (\bar{P})(\chi_{.05}^2/\nu) \quad (19)$$

where \bar{P} is the mean cospectral intensity between the peak and trough, $\chi_{.05}^2/\nu$ is the chi-square value at the .05 level for ν degrees of freedom ($\nu = 2N/m - 1/2 \approx 12$). According to Panofsky and Brier [4, p. 55] the limiting value of $\chi_{.05}^2/\nu = 1.75$.

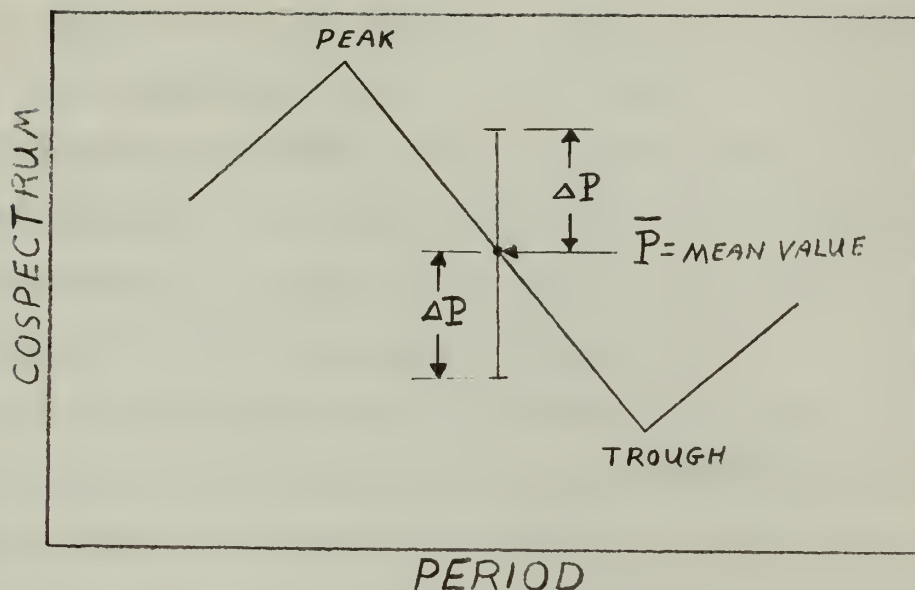


Fig. 1. Illustration of the χ^2/ν test of significance at the 95% level of belief.

A second source of error which may considerably bias the accuracy of cospectral estimates is a phenomenon called "aliasing". This phenomenon removes energy from higher frequencies than those sampled, and may convert it to lower frequencies. Fig. 2 illustrates how aliasing may occur.

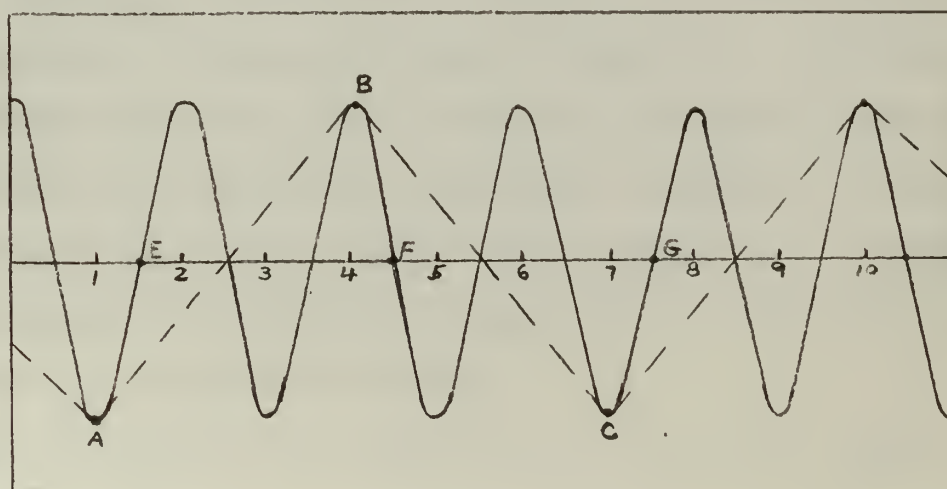


Fig. 2. Illustration of the effects of sampling variations in giving an aliased spectrum.

Suppose a periodic function, such as that illustrated in fig. 2, exists for both $u(t)$ and $v(t)$, and consider the period of the oscillation shown to be $2\Delta t$. If lags are taken at intervals of $3\Delta t$, one is investigating the cospectral estimate at a period of $6\Delta t$. If the sampling times corresponded to points A, B, and C, one obtains a rather large "aliased" cospectral estimate for the period $6\Delta t$. However, if the sampling points had been E, F, and G, the aliased cospectral contribution at period $6\Delta t$ would be zero. Note that the oscillation could be a real atmospheric oscillation or meteorological "noise" of an observational character. The primary atmospheric oscillations of periods shorter than one day are the semi-diurnal (12-hr) wave and a 10.5-hr wave, originally described by Pekeris [5]. However, the amplitude of these waves is quite small.

Blackman and Tukey [1] have shown that the frequencies which are the principal aliases of frequency f_n are $2f_m \pm f_n$, $4f_m \pm f_n$, $6f_m \pm f_n$, etc., where $f_m = 1/2\Delta t$ is the Nyquist frequency. However, the effect of aliasing is most pronounced at frequencies f_n near the Nyquist frequency. Griffith et al [2] suggest that one way of eliminating aliasing from the cospectrum is to delete the cospectral estimates for the last 20 to 40 per cent of the higher frequencies. However, an experiment was performed, using data for Sault Ste. Marie, to assess the extent of aliasing.

Fig. 3 shows three cospectra for Sault Ste. Marie based on:

- (a) the 1500 GMT reports at 24-hr intervals (curve A),

- (b) the 0300 GMT reports at 24-hr intervals (curve B),
and
- (c) both the 0300 GMT and 1500 GMT reports at 12-hr
intervals (curve C).

It may be noted from fig. 3 that all cospectral estimates at periods greater than 2.73 days are in fairly close agreement. However, curves A and B deviate rather markedly at their Nyquist frequency of $\frac{1}{2}$ cycle / day.

In the case of curve C there should be little or no aliasing at periods greater than two days according to Griffith's criterion, since 50 per cent of the spectrum lies between the periods one and two days. On the other hand, at all other stations it will be assumed, henceforth, that all cospectral estimates at periods 2.73 days or larger are relatively unaffected by aliasing.

THE UNIVERSITY OF CHICAGO PRESS

CHICAGO, ILL. 60607

THE UNIVERSITY OF CHICAGO PRESS
1207 EAST 59TH STREET
CHICAGO, ILL. 60637
TEL. (312) 835-5000
FAX (312) 835-5001
WWW.UCHICAGO.PRESS.EDU

THE UNIVERSITY OF CHICAGO PRESS
1207 EAST 59TH STREET
CHICAGO, ILL. 60637
TEL. (312) 835-5000
FAX (312) 835-5001
WWW.UCHICAGO.PRESS.EDU

5. Interpretation of Cospectra

Figs. 3 through 6 present the six cospectra computed for this study. In these figures the ordinate is the cospectrum and the abscissa, plotted for convenience on a logarithmic scale, is the period.

In assessing the reality of the various peaks observed in fig. 3, the procedure embodied in equation (19) will be applied only to curve C, as the other two curves do not deviate significantly except at a period of 3.75 days, which will be discussed separately. In order to compute a mean cospectral estimate for the peak at a period of 10 days, it was assumed that the cospectral estimate at 30 days is the apex of a trough. Inspection of the 95% and 5% fiducial limits established from the mean cospectral values on each side of the peak and trough, indicate that the peaks and trough associated with periods 10 and 6 days, respectively, are significant. The peaks and troughs have only a 5% probability of randomly exceeding these limits; therefore both are considered to be real.

In the case of curve A, the peak appears not to be significantly different when compared to the fiducial limits computed for curve C. However, limits computed from mean values of curve A, although not shown here in order to avoid confusion with those of curve C, show the value at the peak on curve B is considerably greater than the limit to the left side and slightly greater than the limit to the right side. Although the peaks at 3.75 days are not markedly significant from the limit on the right side, there is

justification for stating these peaks seem to be real when one considers both the left and right side limits. Using the significance test discussed above, the reality of any minor peaks in fig. 3 at periods of 3 days or less is doubtful.

The curve in fig. 4 is the average cospectrum for Caribou during the period 1 December 1955 to 28 February 1956. A one-day interval between data points was used to compute this cospectrum. An inspection of the fiducial limits shown in fig. 4 indicates that the peak at 6 days is significantly different from the limits on both the left and right side of the peak, and it is therefore considered to be real. As to the small peak at approximately 3.3 days, the confidence interval shown to the left is quite representative for this peak. It can therefore be concluded that this peak (at 3.3 days) is probably not real, as it does not lie beyond the confidence range. However, it can not be inferred from this that the peak is a result of sampling variations, since the test does not with certainty disprove the reality of the peak.

The curve in fig. 5 is also for Caribou, but was computed from data taken during the winter previous to that used in fig. 4. The limits in this case show the trough and peak at 7.5 and 5 days, respectively, to be real. The trough at 3.75 days is questionable, since it is not significantly different from the limit to the right.

One of the more striking features in each of the cospectra is the large transport associated with the longest

period and the fact this transport has the same sign as the total transport.

In general it is difficult to associate a particular period of the cospectrum with a specific space wave, since the period is a function of both the wavelength and speed of the space wave. It, thereby, seems possible for a transport at a specific period to have contributions from both long and short space waves. This would be the case if the ratio of their wavelengths is equal to the ratio of their speeds. However, assuming that the Rossby wave equation gives a valid relationship between the wave speed and wavelength for any given mean zonal wind, it may be expected that long space waves move eastward slowly and short ones more rapidly. In view of this assumption, the transport associated with a period of thirty days may be attributed to the contributions from long space waves.

Furthermore, large values of transport by the longest period were to be expected, for an examination of the monthly mean 500-mb charts of December 1955 through 1956 showed Sault Ste. Marie and Caribou were on the western side of a mean long wave trough, hence the net transport would most likely be southward (negative). However, for the second cospectrum at Caribou (fig. 5), the period December 1954 through February 1955 was selected by ascertaining through monthly mean 500-mb charts that Caribou was east of the trough and a northward (positive) transport could be expected. In the case of Athens, Georgia, the main reason for selecting this station to provide a comparative

cospectrum is the fact it is almost due south of Sault Ste. Marie. One could expect these two stations to have a net transport of the same sign, but examination of the monthly mean 500-mb charts show the mean long wave trough to have a southwest to northeast tilt of sufficient magnitude to place the trough west of Athens. As a result the net transport for Athens was northward, while that of Sault Ste. Marie was southward. The indicated convergence of momentum transports should then act in such a way as to increase the mean zonal westerlies. Note also that the only pronounced peak in the cospectrum at Athens occurs at a period of 30 days, and that the cospectral values diminish with decreasing period. This is probably due to the fact that short period waves do not penetrate appreciably into this latitude belt.

Interpretation of significant transports associated with shorter periods requires reference to the earlier statement, that short waves are likely to move rapidly. In view of this concept the momentum transport evident near periods of four days is attributed to waves of approximate space-wave numbers 6 to 10, which Saltzmann and Fleisher [6] have called "cyclone waves". However, the momentum transport peaks at periods near 10 days are presumably due to long waves of space-wave numbers 1 to 5.

6. Conclusions

It may be concluded, tentatively, from the cospectra presented in figs. 3 through 6 and the preceding discussion that:

(a) Maximum transport of geostrophic relative angular momentum is accomplished by disturbances with the longer periods.

(b) The peaks with periods near 10 days are related to long space waves.

(c) The direction of the net transport is highly dependent on the position of the mean long wave trough relative to the observing station.

(d) Cyclone waves of space-wave numbers 6 to 10 may contribute to the maximum momentum transports associated with periods near 4 days.

(e) The maximum transports at periods of 30 days may be attributed to the circulation index cycle.

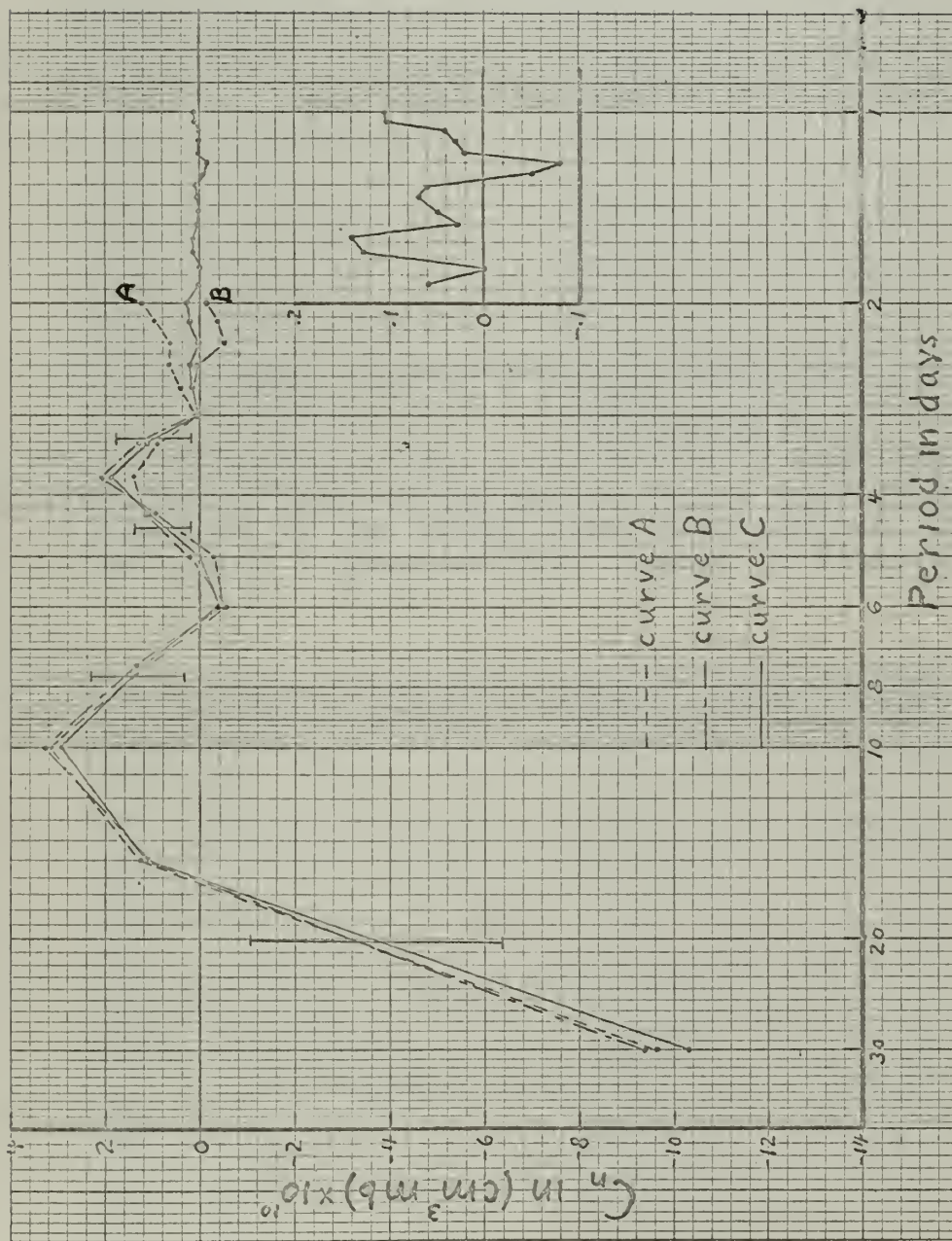


Fig. 3 The cospectrum of the mean relative angular momentum transport at the 500-mb level over Sault Ste. Marie, Michigan for the period 1 December 1955 through 28 February 1956. The auxiliary graph has the ordinate enlarged 100 times for periods 1 to 2 days.



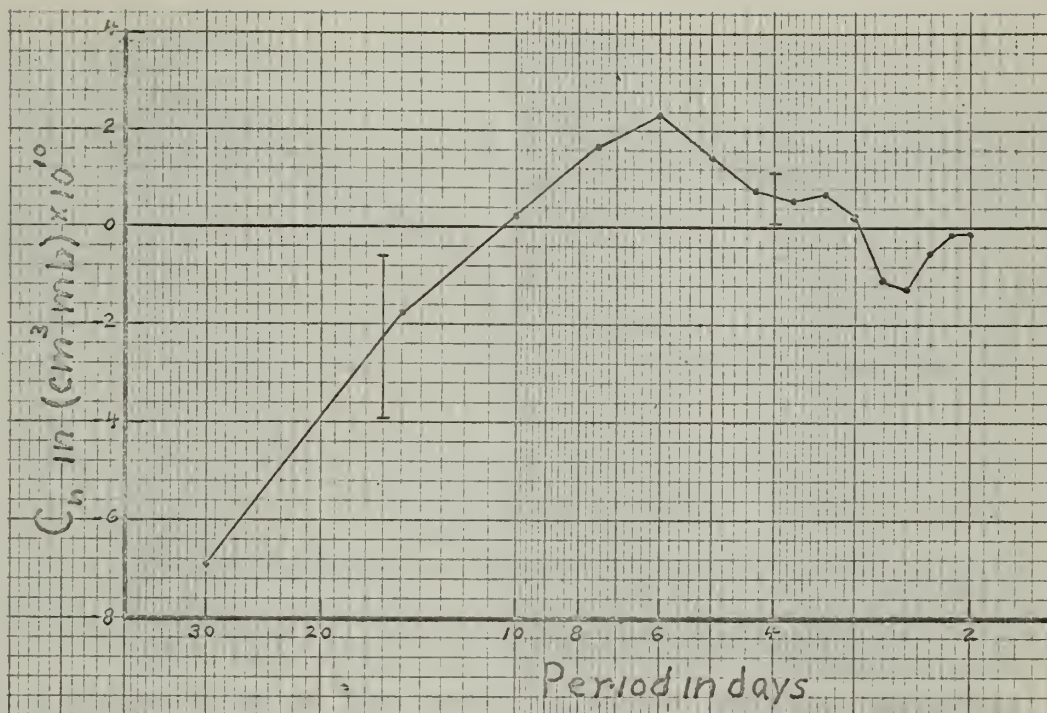


Fig. 4 The cospectrum of the mean relative angular momentum transport at the 500-mb level over Caribou, Maine for the period 1 December 1955 through 28 February 1956.

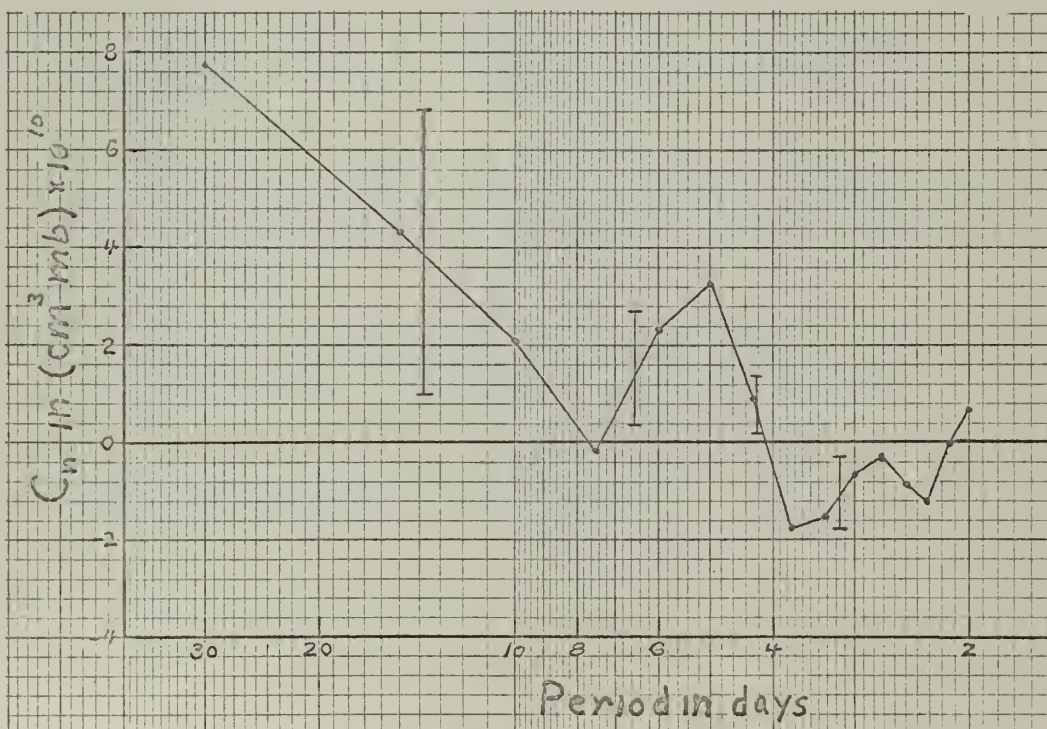


Fig. 5 The cospectrum of the mean relative angular momentum transport at the 500-mb level over Caribou, Maine for the period 1 December 1954 through 28 February 1955.

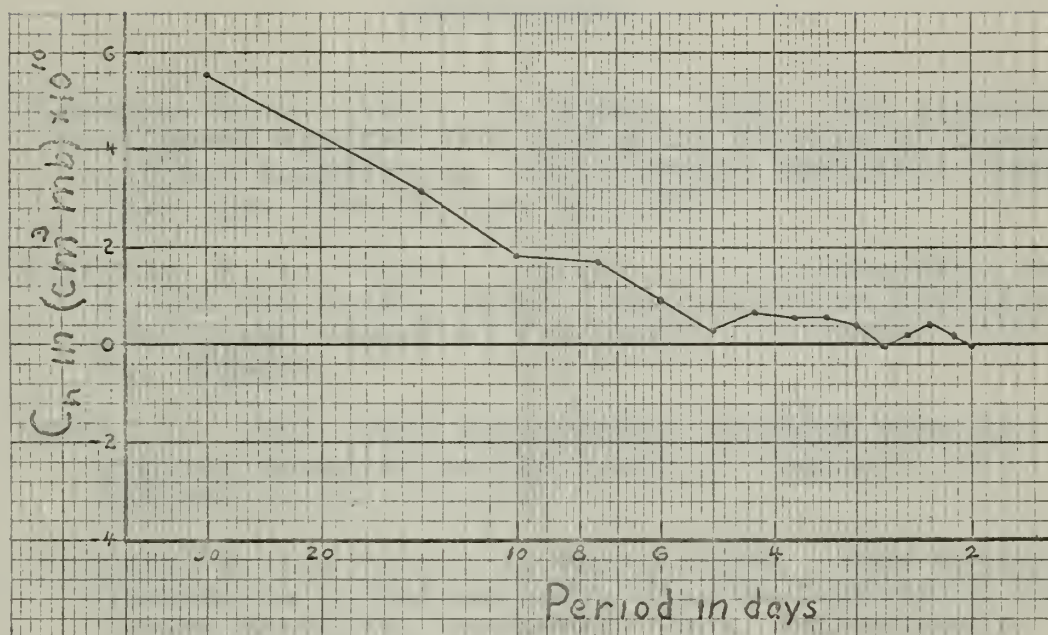


Fig. 6 The cospectrum of the mean relative angular momentum transport at the 500-mb level over Athens, Georgia for the period 1 December 1955 through 28 February 1956.

BIBLIOGRAPHY

1. Blackman, R. B., and J. W. Tukey, 1958: The measurement of power spectra from the point of view of communications engineering. Bell System Technical Journal, 37.1, pp. 185-282, pp. 485-570.
2. Griffith, H. L., Capt., U.S.A.F., H. A. Panofsky, and I. Van der Hoven, 1956: Power-Spectrum analysis over large ranges of frequency. J. Meteor., 13, pp. 279-282.
3. Mintz, Y., 1951: The geostrophic poleward flux of angular momentum in the month of January, 1949. Tellus, 3, pp. 195-200.
4. Panofsky, H. A., and G. L. Brier, 1958: Some Application Statistics to Meteorology, Mineral Industries Extension Services, University Park, Pennsylvania.
5. Pekeris, C. L., 1937: Atmospheric oscillations, Proc. Roy. Soc. A, 158, pp. 650-671.
6. Saltzman, B. and A. Fleisher, 1960: The exchange of kinetic energy between larger scales of atmospheric motion. Tellus, 12, pp. 375-377.
7. Starr, V. P., 1951: A note on the eddy transport of angular momentum. Quart. J. R. Met. Soc., 77, pp 44-48.
8. U. S. Weather Bureau, 1955-56: Daily Series Synoptic Weather Maps, Northern Hemisphere Sea Level and 500 Millibar Charts, December 1955 to February 1956, inclusive.
9. U. S. Weather Bureau, 1955-56: Daily Series Synoptic Weather Maps, Northern Hemisphere Data Tabulations, December 1955 to February 1956, inclusive.
10. Widger, W. K., 1949: A study of the flow of angular momentum in the atmosphere. J. Meteor. 6, pp. 291-299.

APPENDIX I

Derivation of the Cospectral Function

The cross covariance at lag τ , of two functions of time, is given by

$$\begin{aligned} S(\tau) &= \lim_{T \rightarrow \infty} \frac{1}{T} \int_0^T u(t) \cdot v(t+\tau) dt \\ &= \lim_{T \rightarrow \infty} \frac{1}{T} \int_0^T \left[\sum_n A_n \cos\left(\frac{2\pi n t}{T} + \theta_n\right) \right] \left[\sum_m B_m \cos\left(\frac{2\pi m (t+\tau)}{T} + \psi_m\right) \right] dt \\ &= \lim_{T \rightarrow \infty} \frac{1}{T} \int_0^T \sum_n \sum_m A_n B_m \left[\cos\left(\frac{2\pi n t}{T} + \theta_n\right) \cos\left(\frac{2\pi m t}{T} + \frac{2\pi m \tau}{T} + \psi_m\right) \right] dt \\ &= \lim_{T \rightarrow \infty} \frac{1}{T} \int_0^T \sum_m \sum_n \frac{A_n B_m}{2} \left\{ \cos\left[\frac{2\pi (m+n)t}{T} + (\psi_m + \theta_n) + \frac{2\pi n \tau}{T}\right] \right. \\ &\quad \left. + \cos\left[\frac{2\pi (m-n)t}{T} + (\psi_m - \theta_n) + \frac{2\pi m \tau}{T}\right] \right\} dt \end{aligned}$$

The first cosine term integrates to zero for all cases $m, n \neq 0$. The second cosine term integrates to zero for all cases $m \neq n$. When $m = n$, integration gives

$$\begin{aligned} S(\tau) &= \lim_{T \rightarrow \infty} \sum_{n=0}^{\infty} \frac{A_n B_n}{2T} \left\{ \cos\left[(\psi_n - \theta_n) + \frac{2\pi n \tau}{T}\right] \right\} \\ S(\tau) &= \lim_{T \rightarrow \infty} \sum_{n=0}^{\infty} \frac{A_n B_n}{2T} \left[\cos(\psi_n - \theta_n) \cos \frac{2\pi n \tau}{T} - \sin(\psi_n - \theta_n) \sin \frac{2\pi n \tau}{T} \right] \\ S(\tau) &= \lim_{T \rightarrow \infty} \sum_{n=0}^{\infty} \frac{A_n B_n}{2T} \left[\cos(\psi_n - \theta_n) \cos \frac{2\pi n \tau}{T} - \sin(\psi_n - \theta_n) (-\sin \frac{2\pi n \tau}{T}) \right] \end{aligned}$$

The evenized cross covariance equals one-half the sum of the cross covariance at τ and $-\tau$,

$$\hat{S}(\tau) = \frac{S(\tau) + S(-\tau)}{2} = \lim_{T \rightarrow \infty} \sum_{n=0}^{\infty} \frac{A_n B_n}{2T} \cos(\psi_n - \theta_n) \cos \frac{2\pi n \tau}{T} \Delta n; \Delta n = 1, 2, \dots$$

Defining the unsmoothed cospectrum as

$$C(n) = \lim_{T \rightarrow \infty} \frac{A_n B_n}{2T} \cos(\psi_n - \theta_n)$$

the Fourier transform of $C(n)$ is obtained as

$$S(\tau) = \int_0^{\infty} C(n) \frac{2\pi n \tau}{T} dn$$

Multiplying both sides by $\cos \frac{2\pi n \tau}{T} d\tau$ and integrating from 0 to T gives

$$\lim_{T \rightarrow \infty} \int_0^T S(\tau) \cos \frac{2\pi n \tau}{T} d\tau = \lim_{T \rightarrow \infty} \int_0^T C(n) \left(\frac{1}{2} + \frac{4\pi n \tau}{T} \right) d\tau$$

For all $n \neq 0$, $\cos \frac{4\pi n \tau}{T}$ integrates to zero, giving

$$C(n) = 2 \lim_{T \rightarrow \infty} \int_0^T S(\tau) \cos \frac{2\pi n \tau}{T} d\tau$$

where Γ is the integration limit and T is the fundamental period.

THE UNIVERSITY OF CHICAGO

PHYSICS DEPARTMENT

RECEIVED 1964 JAN 15 10 10 AM

FROM THE PHYSICS DEPARTMENT

TO THE PHYSICS DEPARTMENT

RE: [illegible]

DATE: 1964 JAN 15

thesB5459

A study of geostrophic angular momentum



3 2768 002 13522 0

DUDLEY KNOX LIBRARY